Electronic Supplementary Material (ESI) for Integrative Biology.

Supplemental Figure 1: Fluorescence lifetime imaging microscopy (FLIM) measures chromatin condensation state of PicoGreen-stained nuclei, similar to Figure 4. (A) Frequency distribution of the spatial distributions of mean fluorescence lifetimes for the three treatment conditions. Error bars reflect SEM. (B) Wide-field fluorescence images (left) and mean fluorescence lifetime heat maps (right) of HUVECs with PicoGreen-stained DNA and either untreated or treated with TSA. 30-60 nuclei were segmented per treatment and quantified for mean fluorescence lifetime (C) and variance of the mean lifetime (D). Treatment with TSA resulted in global chromatin decondensation as evinced by a statistically significant increase in mean fluorescence lifetime ($p<0.001$) and a statistically significant reduction in the variance of the mean fluorescence lifetime (C, $p<0.001$). Scale bar is 10 μm. Error bars reflect SEM.

Supplemental Figure 2: FLIM of blebbistatin treated nuclei. The mean fluorescence lifetimes of HUVECs with Hoechst 33342-stained DNA for untreated controls, a DMSO control for TSA treatment, a DMSO control for blebbistatin treatment and blebbistatin treatment. Individual nuclei were segmented for calculation of the mean fluorescence lifetime. There was no statistically significant change in mean fluorescence lifetime ($p>0.05$). 30-60 nuclei were segmented per treatment and quantified for mean fluorescence lifetime. Error bars reflect SEM.

Supplemental Figure 3: Transfection of RFP-KASH constructs in HUVECs. Images from live-cell experiments of a HUVEC transfected with either (A) the exogenous dominant negative KASH construct RFP-KASH or (B) the exogenous control KASH construct RFP-KASH-ΔL which lacks the luminal SUN binding domains and therefore does not displace the nesprin proteins from the nuclear envelope (indicated with arrows). (A) The RFP-KASH construct shows increased fluorescence intensity at the nuclear envelope compared with no nuclear envelope localization for the RFP-KASH-ΔL construct (B).

Supplemental Figure 4: Extended MSD plots from particle-tracking measurements. (A) MSD versus lag time plots of ten individual control cells. (B) Extended plot of Figure 6 containing error bars to show their magnitudes for comparison. Error bars reflect SEM.

Supplemental Discussion: Nuclear viscoelasticity from particle tracking.
Determining cellular rheology from particle tracking experiments requires consideration of numerous factors. For equilibrium systems, viscoelasticity manifests as anomalous subdiffusion with $MSD \sim \tau^{\beta}$ and $0<\beta<1$[1]. Material viscoelasticity, binding and obstruction[2] as well as overcrowding[3] similarly form the basis for anomalous subdiffusion in active cellular systems. However, cells are not equilibrium systems; motor protein activity enhances diffusive motion within cells beyond that of simple thermal fluctuations as part of a phenomenon termed “active

diffusion"[4, 5]. Previous studies have shown these motors are stochastic and essentially isotropic, making them similar in form to the thermal energy-derived fluctuations[6, 7]. Thus, they act to globally and nonspecifically increase the time-dependence of these random fluctuations much like a forcing function, thereby driving this motion beyond that of simple thermal agitation[5-7].

Our results highlight the role of ATP-dependent motor activity in enhancing nuclear diffusive motion and chromatin fluctuations as measured through β.The long time scales (low frequency) of these experiments allows visualization of motor activity on time-dependent influence, as shown previously[8]. In particular, we show myosin II activity on the actin cytoskeleton significantly enhances these superthermal fluctuations within the nucleus through the LINC complex. The presence of the vast force-generating apparatus of the cytoskeleton likely explains why our results deviate in behavior from a recent study of chromosomal fluctuations in bacteria and yeast cells devoid of a comprehensive cytoskeleton that exhibited a lower diffusive exponent in control cells and where ATP depletion manifests itself solely in the prefactor[4].

By contrast, our work shows chromatin condensation state primarily impacts the prefactor. For typical polymeric systems, modulation of polymer viscoelasticity would affect the exponent, transitioning from elastic ($\beta \rightarrow 0$) to viscous contributions ($\beta \rightarrow 1$) or *vice versa*[1]. Yet, our work shows that changes to chromatin condensation have a limited impact on β, which we suggest stems from active forces playing the dominant role in modulating β[1, 8] (as discussed above). Additionally, the seemingly infinite mechanisms of stress dissipation by the intranuclear polymer network (including a wide distribution of intermediate and metastable conformations for chromatin, DNA and its binding partners as well as a distribution of binding residence times) results in the characteristic power-law behavior and the absence of any characteristic timescales of relaxation[9]. Thus, the time-dependent effect of altering intranuclear polymer network mechanics would necessarily have a lesser impact on the time dependence of network fluctuations than in classical homogenous polymeric systems.

Previous studies have highlighted that probes bound to a percolated network are capable of capturing network dynamics and mechanics for *in vitro* biopolymer systems[10, 11], including behavior relevant to the study of mechanobiology. The use of bound probes and the presence of active motors (creating nonequilibrium systems) results in invalidation of the Generalized Stokes-Einstein Relation (GSER) for calculation of the classical material properties. However, in place of the GSER the use of bound probes makes pertinent several models of polymer dynamics for qualitative analysis, including the Rouse chain model and the de Gennes model of reptation depicting polymer dynamics in a crowded environment[12, 13]. Conceptually, changes to local chromatin condensation state and organization can be thought of as altering the effective "tube size" for this reptation[12] which act to change the amplitude of such movements[13], whereas the motors would primarily affect the time dependence and its enhancement beyond simple thermal agitation. However, it is important to note that the application of these models is convenient to consider these phenomena conceptually, but their use is neither exact nor definitive. Nonetheless, while determination of the classical material properties is no longer straightforward through the

GSER, particularly given the material heterogeneity, D_{eff} still serves as an indicator of material properties for these network fluctuations in a manner conceptually similar to these polymer dynamic models, essentially as an inverse to effective resistance. For our experiments increased D_{eff} reflects a reduced resistance to motion that accompanies the chromatin decondensation and *vice versa*[9, 14, 15]. We further show the link between chromatin condensation state and D_{eff} using FLIM[16].

In summation, there are numerous physical and biological limitations that limit determination of viscoelastic properties from particle tracking microrheology. As such, in this work we have not provided a direct extrapolation of viscoelasticity from measurements of intranuclear fluctuations, particularly given the long time steps required to measure small intranuclear movements. This work provides useful comparative data of chromatin condensation and force generation and propagation. However, more appropriate mechanical measurements – such as cell stretching[15], micropipette aspiration[9, 14], compression[17], etc. – can be used to quantify absolute material properties.

1. J. C. Crocker and B. D. Hoffman, *Cell Mechanics*, 2007, **83**, 141-178.
2. M. J. Saxton, *Biophysical journal*, 2007, **92**, 1178-1191.
3. M. Weiss, M. Elsner, F. Kartberg and T. Nilsson, *Biophysical journal*, 2004, **87**, 3518-3524.
4. S. C. Weber, A. J. Spakowitz and J. A. Theriot, *Proceedings of the National Academy of Sciences of the United States of America*, 2012, **109**, 7338-7343.
5. C. P. Brangwynne, G. H. Koenderink, F. C. MacKintosh and D. A. Weitz, *Trends in cell biology*, 2009, **19**, 423-427.
6. A. W. C. Lau, B. D. Hoffman, A. Davies, J. C. Crocker and T. C. Lubensky, *Physical review letters*, 2003, **91**.
7. A. W. C. Lau and T. C. Lubensky, *Phys Rev E*, 2009, **80**.
8. B. D. Hoffman, G. Massiera, K. M. Van Citters and J. C. Crocker, *Proceedings of the National Academy of Sciences of the United States of America*, 2006, **103**, 10259-10264.
9. K. N. Dahl, A. J. Engler, J. D. Pajerowski and D. E. Discher, *Biophysical journal*, 2005, **89**, 2855-2864.
10. J. L. McGrath, J. H. Hartwig and S. C. Kuo, *Biophysical journal*, 2000, **79**, 3258-3266.
11. M. T. Valentine, Z. E. Perlman, M. L. Gardel, J. H. Shin, P. Matsudaira, T. J. Mitchison and D. A. Weitz, *Biophysical journal*, 2004, **86**, 4004-4014.
12. I. Bronstein, Y. Israel, E. Kepten, S. Mai, Y. Shav-Tal, E. Barkai and Y. Garini, *Physical review letters*, 2009, **103**, 018102.
13. H. Hajjoul, J. Mathon, H. Ranchon, I. Goiffon, J. Mozziconacci, B. Albert, P. Carrivain, J. M. Victor, O. Gadal, K. Bystricky and A. Bancaud, *Genome Res*, 2013, **23**, 1829-1838.
14. J. D. Pajerowski, K. N. Dahl, F. L. Zhong, P. J. Sammak and D. E. Discher, *Proceedings of the National Academy of Sciences of the United States of America*, 2007, **104**, 15619-15624.
15. K. J. Chalut, M. Hopfler, F. Lautenschlager, L. Boyde, C. J. Chan, A. Ekpenyong, A. Martinez-Arias and J. Guck, *Biophysical journal*, 2012, **103**, 2060-2070.
16. D. Lleres, J. James, S. Swift, D. G. Norman and A. I. Lamond, *Journal of Cell Biology*, 2009, **187**, 481-496.
17. K. M. Stroka and H. Aranda-Espinoza, *Cellular and molecular bioengineering*, 2011, **4**, 9-27.

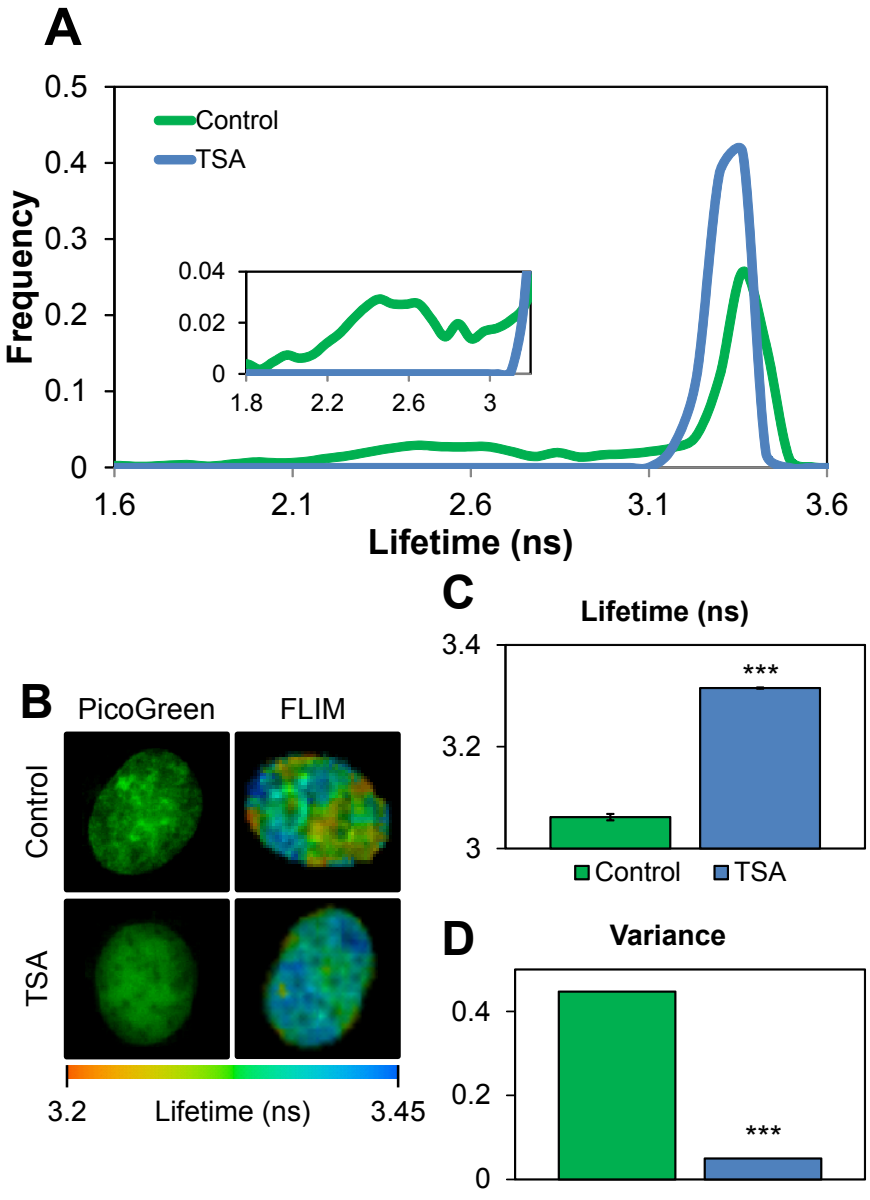
A
0.5
0.4
0.3
0.2
0.1
0
Frequency
Control
TSA
0.04
0.02
0
1.8
2.2
2.6
3
1.6
2.1
2.6
3.1
3.6
Lifetime (ns)
B
PicoGreen
FLIM
Control
TSA
3.2
Lifetime (ns)
3.45
C
Lifetime (ns)
3.4
3.2
3
***
Control
TSA
D
Variance
0.4
0.2
0
***

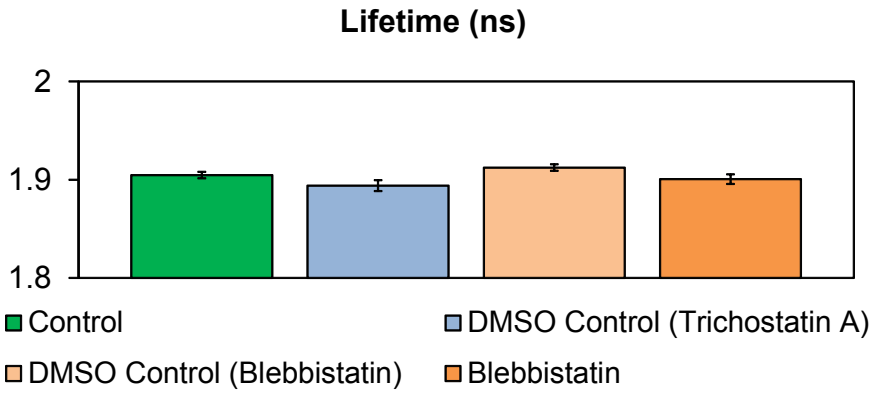
Lifetime (ns)
2
1.9
1.8
Control
DMSO Control (Trichostatin A)
DMSO Control (Blebbistatin)
Blebbistatin

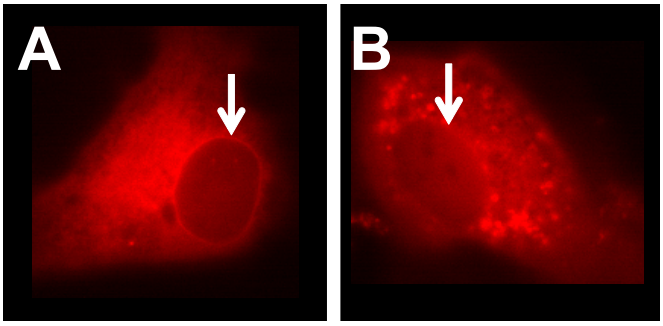
A
B

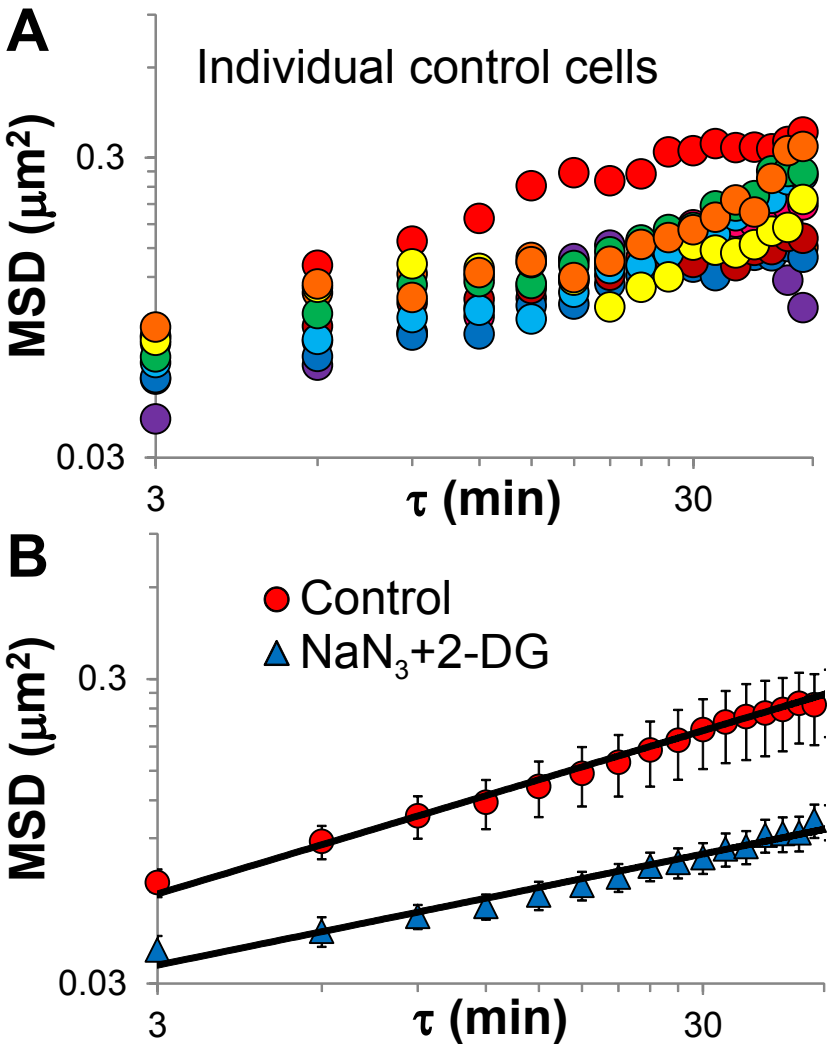
A
Individual control cells
MSD (μm²)
0.3
0.03
3
τ (min)
30
B
Control
NaN3+2-DG
MSD (μm²)
0.3
0.03
3
τ (min)
30